JOURNAL OF MATERIALS SCIENCE **36** (2001) 811–814

Phonon dispersion and elastic constants in Fe-Cr-Mn-Ni austenitic steel

S. A. DANILKIN*
Institute for Physics and Power Engineering, 249020 Obninsk, Russia
E-mail: danilkin@ippe.obninsk.ru

H. FUESS, T. WIEDER
Technische Universität Darmstadt, 64287 Darmstadt, Germany
E-mail: wieder@hrzpub.tu-darmstadt.de

A. HOSER
Hahn-Meitner-Institut, 14109 Berlin, Germany

The lattice dynamics of Fe-18Cr-10Mn-16Ni austenitic steel was studied by inelastic neutron scattering techniques. Phonon dispersion curves were measured in the [100], [011] and [111] directions at low wavevectors. The measured dispersion curves are similar to those of the γ-Fe and the $Fe_{0.75}Ni_{0.25}$ alloy, but do not show the anomalous concave curvature of the T_1 [001] branch at lower wave vectors as characteristic for γ-Fe. All available data were used for the evaluation of the atomic force constants, elastic constants and engineering elastic moduli of Fe-18Cr-10Mn-16Ni steel.

1. Introduction

Nitrogen stabilises the FCC austenitic structure at low temperatures and during cold working, improves the strength and corrosion resistance. In order to understand the effect of the interstitial nitrogen and metallic alloying components on the interatomic bonding in austenitic steels, the elastic moduli and vibrational frequency distributions of nitrogen austenitic polycrystalline alloys were studied previously by an ultrasonic method [1] and by neutron spectroscopy [2]. All experiments made up to now show the complicated effect of alloying components and interstitial nitrogen on the Me-Me interatomic bonding in austenitic steels. A theoretical description based on a model using continuum elasticity is in disagreement with experimental data. Apparently other factors than elastic misfit enter into the problem.

The bulk and shear moduli of polycrystalline steels studied in paper [1] are the average over the aggregates of the crystallites and are defined as an average of the elastic constants C_{ij}. Similar to elastic moduli, the vibrational frequency distribution is sum of all normal modes of vibrations over the Brillouin zone. This distribution provides integral parameters related to the interatomic interactions, namely the Debye temperature and the second moment of the metal atom frequency distribution. The atomic force constants are connected with the measured frequency distribution in a rather complicated non-analytical way and it is difficult to apply models of lattice dynamics to calculate these constants. In contrast to the polycrystalline case, the evaluation of the spectroscopic data is considerably easier for single crystal samples. In this case the phonon dispersion curves ($\omega = \omega(\mathrm{s}, \boldsymbol{q})$, s-polarisation, $\boldsymbol{q}$-phonon wave vector) provide information on the Me-Me interatomic force constants and the elastic constants C_{ij} which are related to the low-frequency part (elastic limit) of the dispersion curves.

Up to now, acoustic branches along the [110] direction and the L-branch along the [100] direction have been measured in Fe-18Cr-10Mn-16Ni steel [3] and in Fe-19Cr-11Mn-15Ni steel [4] (Fig. 1). The present study relates to the phonon dispersion along the [100] and the [111] direction in the Fe-18Cr-10Mn-16Ni steel. Here we report on our measurements for the steel without nitrogen. Because the energy range of the spectrometer was limited by the low-energy transfers, we focused on the measurements of phonons with low-q wavevectors ($q \approx 0.03 \div 0.15$). All available experimental data have been used to fit the parameters of model of the lattice dynamics. Further, the elastic constants C_{ij} and engineering elastic moduli B and G were calculated in the low-q limit. They were compared with the data on the elastic constants of γ-Fe [5], Fe-Ni [6] and Fe-Cr-Ni alloys [7].

2. Experimental

A single crystal of Fe-18Cr-10Mn-16Ni steel (0.08 C, 18.48 Cr, 16.13 Ni, 9.64 Mn, 0.45 Si, 0.004 S, 0.008 P, Fe-balance, wt.%) was grown by Brigdman method at Tomsk State University. The sample was

*Author to whom all correspondence should be addressed.

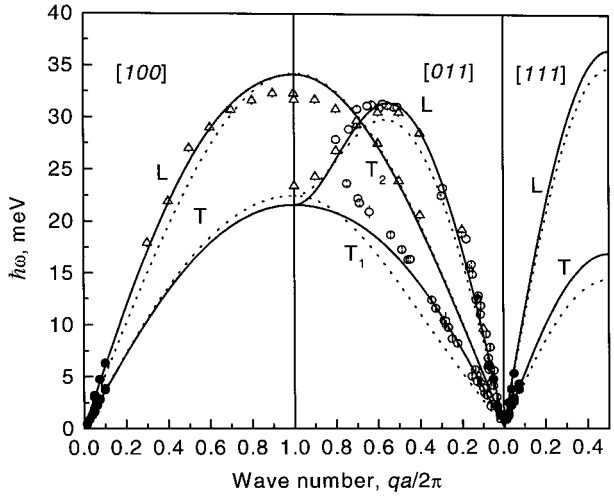

Figure 1 Dispersion curves of Fe-18Cr-10Mn-16Ni steel. • - present work, ○ - experiment [3], Δ - experiment [4]. Solid line – fit of all data to the CPP model of lattice dynamics, dots – calculations for γ-Fe [13].

$8 \times 8 \times 40$ mm^3 in size with the longer dimension along the [100] direction. The lattice parameter and mosaic spread of the single crystal was found to be $a = 0.359$ nm and $\delta\vartheta \approx 30'$ correspondingly. During the measurements the crystal was aligned to have the (110) plane coinciding with the scattering plane defined by the wavevectors of the incident and scattered neutrons $-\boldsymbol{k_0}$ and $\boldsymbol{k}$. The measurements were performed by the triple-axis spectrometer E1 at the Hahn-Meitner-Institut, Berlin [8]. Pyrolitic graphite PG (002) reflections were used for the monochromator and analyser crystal. The collimations were $40' - 20' - 20' - 40'$ or $40' - 40' - 40' - 40'$. The phonons were measured in constant-Q mode with fixed incident wavelength of 0.2426 nm.

3. Results and discussion

The measured phonons are shown in Fig. 1 together with the data of the previous studies [3, 4]. The results obtained with the E1 spectrometer in [011] direction are in good agreement with low-q data measured using the time-of-flight spectrometer [3]. In the [100] and [111] direction, the obtained data fill gaps in the available data and allow deriving the parameters of the interatomic interactions in steel. The dispersion curves of Fe-18Cr-10Mn-16Ni steel are similar to those of γ-Fe measured at 1428 K [5] and $Fe_{0.7}Ni_{0.3}$ alloy [6] (Fig. 1). The notable difference with γ-Fe is in the behaviour of the T_1 [011] branch. In this direction phonon frequencies in γ-Fe are lower at all q and show anomalous concave curvature at lower wave vectors (Fig. 1). The frequencies of L the [100] and T [111] branches in γ-Fe are also lower but do not show this anomalous behaviour.

To evaluate the atomic force constants, the experimental data were analysed by a central pair potential model (CPP) [9] taking into account interactions between the first and the second neighbours in FCC lattice. In this case there are four free parameters which are the first and second derivatives of interatomic pair-wise potential $V(r)$:

$$\beta_n = V''(r_n) \text{ and } \alpha_n = V'(r_n)/r_n \qquad (1)$$

where r_n, is the interatomic distance ($n = 1$, 2 is the neighbour's number). Force constant β_n relates to bond-stretching forces. The constant α_n represents the bond-bending forces, which are characteristic not only for the CPP model of the lattice dynamics, but appear similarly, for instance, in the axial symmetrical model [10] and in the non-central model of de-Launay [11].

Typical expressions for the elements of the dynamical matrix $D_{i,j}$ (i, $j = 1$, 2 or 3) in the CPP model are [12]:

$$\begin{aligned} D_{1,1}(\vec{q}) &= 4\beta_1 + 8\alpha_1 - 2(\beta_1 + \alpha_1)C_1(C_2 + C_3) \\ &\quad - 4\alpha_1 C_2 C_3 + 4\beta_2 S_1^2 + 4\alpha_2\left(S_2^2 + S_3^2\right), \\ D_{1,2}(\vec{q}) &= 2(\beta_1 - \alpha_1)S_1 S_2 \end{aligned} \qquad (2)$$

where $C_i = \cos(aq_i/2)$, $S_i = \sin(aq_i/2)$, with a-lattice parameter.

The eigenvalues of the dynamical matrix are products $M\omega_s(\boldsymbol{q})$, where s denotes the polarisation of phonons with frequency ω and wave vector $\boldsymbol{q}$. Following the standard procedure, the analytical relations for frequencies were obtained for the phonons in symmetrical directions. Then the interaction parameters α_i and β_i were computed from the experimental data by a least squares fit procedure. Using all experimental data shown in Fig. 1, we obtain the following parameters:

$$\begin{aligned} &\beta_1 = 34.12 \pm 0.06, \quad \alpha_1 = -3.13 \pm 0.04, \\ &\beta_2 = 4.10 \pm 0.05, \quad \alpha_2 = 0.91 \pm 0.04 \text{ N/m}. \end{aligned} \qquad (3)$$

The calculated dispersion curves shown in Fig. 1 are generally in good agreement with the experiment. All low-q data check well with the calculated curves. There is some disagreement with experiment in the L [100], T_1 [011] and T_2 [011] branches at $q = 0.8 \div 1.0$. One notices however, that the experimental frequencies for the T_1 [011] branch at $q = 0.6 \div 0.8$ as measured in [3] seem to be too high to fit the frequency of the longitudinal branch L [011] at the zone boundary reported in paper [4].

We compare the obtained force constants with the corresponding data for γ-Fe. The extended generalised form of the exponential potential developed for γ-Fe in paper [13] yields dispersion curves which are close to experiment (Fig. 1) with the following atomic force constants:

$$\begin{aligned} &\beta_1 = 33.679, \quad \alpha_1 = -2.210, \\ &\beta_2 = -1.454, \quad \alpha_2 = 0.607 \text{ N/m}. \end{aligned} \qquad (4)$$

The values of the atomic force constants β_i and α_i in Fe-18Cr-10Mn-16Ni steel are close to those in γ-Fe, except of β_2 which differs considerably having the opposite sign.

The force constants involved in the dynamical matrix can be related to elastic constants of the alloy by expanding the elements of the dynamical matrix (2) and

finding their limit at $q \to 0$ [9]:

$$aC_{11} = 2\beta_1 + 2\alpha_1 + 4\beta_2,$$
$$aC_{44} = \beta_1 + 3\alpha_1 + 4\alpha_2, \quad (5)$$
$$aC_{12} = \beta_1 - 5\alpha_1 + 4\alpha_2.$$

With the values from (3) for the atomic force constants the elastic constants of Fe-18Cr-10Mn-16Ni steel are:

$$C_{11} = 2.18 \pm 0.01, C_{12} = 1.29 \pm 0.01,$$
$$C_{44} = 0.79 \pm 0.01\, 10^{11}\ \mathrm{N/m^2}. \quad (6)$$

The elastic constants C_{44} and C_{12} are very close with those in γ-Fe: $C_{44} = 0.77$, $C_{12} = 1.22 \cdot 10^{11}$ N/m^2 [5]. However value of C_{11} in γ-Fe ($C_{11} = 1.54 \cdot 10^{11}$ N/m^2) is much lower then in Fe-18Cr-10Mn-16Ni steel. Correspondingly, the phonon branches determined mainly by C_{11} (L [100] and T [111] branches) or by the difference ($C_{11} - C_{12}$) as in the case of the *T2* [011] branch have lower frequencies in γ-Fe.

Notice that the elastic constant C_{11} and C_{12} in FCC Fe-Cr-Ni alloys containing $18 \div 19\%$ Cr and $10 \div 12\%$ Ni lies between $C_{11} = 1.91 \div 2.16\, 10^{11}$ N/m^2 and $C_{12} = 1.91 \div 1.45\, 10^{11}$ N/m^2 [7]. Values of C_{11} and C_{12} obtained for Fe-18Cr-10Mn-16Ni steel are in these ranges, while value of C_{44} (6) is much lower then in Fe-Cr-Ni alloys—$C_{44} = 1.22 \div 1.39\, 10^{11}$ N/m^2. These differences in elastic constants are connected with the effect of alloying additions on the interatomic bonding in iron. In particular, the elastic constants C_{11} and C_{12} in $Fe_{1-x}Ni_x$ alloys show strong increase with increasing nickel content [6]. The value of $C_{11} = 1.46\, 10^{11}$ N/m^2 in $Fe_{0.7}Ni_{0.3}$ is rather close to the corresponding one obtained for γ-Fe [5], while C_{11} in $Fe_{0.25}Ni_{0.75}$ ($C_{11} = 2.30\, 10^{11}$ N/m^2) is approximately equal to C_{11} in pure nickel.

Another important difference between elastic constants of Fe-18Cr-10Mn-16Ni steel and Fe-Cr-Ni alloys [7] is that these alloys having approximately the same C_{12}/C_{11} ratio, show a much lower C_{44}/C_{11} ratio and a much lower elastic anisotropy $A = 2C_{44}/(C_{11} - C_{12})$. These shifts could arise from the manganese, a strong antiferromagentic element, which tends to move the FCC alloy toward the BCC element.

From the elastic constants C_{ij} the bulk and shear modulus was calculated. In cubic crystals the bulk modulus B represents the pure dilatation and is:

$$B = (C_{11} + 2C_{12})/3, \quad (7)$$

yielding $B = 1.59 \pm 0.01 \cdot 10^{11}$ N/m^2. For the shear modulus there are several methods of calculation. In the frame of the Voigt-Reuss-Hill averaging method [14] the shear modulus is:

$$G_H = \frac{(C_{11} - C_{12}) + 3C_{44}}{10} + \frac{5}{2}\left[\frac{4}{(C_{11} - C_{12})} + \frac{3}{C_{44}}\right]^{-1}, \quad (8)$$

yielding $G_H = 0.63 \cdot 10^{11}$ N/m^2. The averaging using Hershey-Kriiner-Eshelby method [7] gives the same value of shear modulus.

The value of the bulk modulus in Fe-18Cr-10Mn-16Ni steel obtained from the atomic force constants is close to that in Fe-20Cr-9Ni-9Mn alloy ($B = 1.51 \cdot 10^{11}$ N/m^2) obtained from ultrasonic data [1]. An extrapolation of the data on nine Fe-Cr-Ni-Mn steels [1] to the composition Fe-18Cr-10Mn-16Ni results in an even better agreement, yielding a value of $B_{\mathrm{ext}} = 1.51 \cdot 10^{11}$ N/m^2. However the shear modulus in Fe-18Cr-10Mn-16Ni steel is 20% lower then in Fe-20Cr-9Ni-9Mn alloy.

4. Conclusion

1. The dispersion curves of the Fe-18Cr-10Mn-16Ni steel are similar to those of the γ-Fe and the $Fe_{0.75}Ni_{0.25}$ alloy, but do not show the anomalous concave curvature of the T_1 [001] branch at lower wave vectors characteristic for γ-Fe.

2. The atomic force constants β_1 and α_1 for the first neighbours and the bond-bending force constant α_2 for the second neighbours of the Fe-18Cr-10Mn-16Ni steel are close to those of γ-Fe, while the bond-stretching force constant β_2 for the second neighbours differs considerably having the opposite sign.

3. The elastic constant C_{44} in Fe-18Cr-10Mn-16Ni steel has a much lower value in comparison with that of Fe-Cr-Ni alloys. Correspondingly, a much lower C_{44}/C_{11} and Zener anisotropy ratio is observed which could arise from the manganese alloying addition.

4. The bulk modulus of Fe-18Cr-10Mn-16Ni steel calculated form the atomic force constants is close to the value measured by the ultrasonic method for Fe-Cr-Ni austenitic alloys, whereas the shear modulus is about 20% lower.

Acknowledgements

This work has been performed in the frame of the Russian Federal Programme "Priority Investigations and developments in Civil Science and Technology." Substantial financial support was provided within a German-Russian co-operation between The German Ministerium für Forschung und Bildung and the Russian Ministry of Science and Technology under the project number DLR RUS 151-97. The European Commission supported the experiments at BENSC in Berlin through the TMR Programme "Access to large-scale facilities."

References

1. S. KIM and H. M. LEDBETTER, *J. Mater Sci.* **29** (1994) 5462.
2. V. G. GAVRILUK, V. M. NADUTOV, S. A. DANILKIN, V. P. MINAEV, S. P. EFIMENRO, A. A. LISHREVICH and V. V. SUMIN, *Mat. Sci. and Eng.* **A203** (1995) 300.
3. S. A. DANILKIN and E. L. JADROWSKI, *Physica B* **234–236** (1997) 900.
4. V. V. SUMIN, in ILL Experimental Reports and Theory Activities, Report No. 7-03-21, 1998.
5. J. ZARESTKY and C. STASSIS, *Phys. Rev.* **B35** (1987) 4500.
6. E. D. HALLMAN and B. N. BROCKHOUSE, *Can. J. Phys.* **47** (1969) 1117.
7. H. M. LEDBETTER, *Phys. Stat. Sol.* (*a*) **85** (1984) 89.

8. E1 Triple-Axis Spectrometer with polarisation analysis, in "Neutron-Scattering Instrumentation at the Research Reactor BER II" (Berlin Neutron Scattering Center–BENSC, May 1996) p. 12.
9. G. LEIBFRIED, Gittertheorie der Mechanischen und Thermischen Eigenschaften der Kristalle, Handbuch der Physik, band VII, teil 2 (Springer-Verlag, Berlin, 1955).
10. G. W. LEHMAN, T. WOLFRAM and R. E. DE-WAMES, *Phys. Rev*. **128** (1962) 1593.
11. J. DE-LAUNAY, *J. Chem. Phys*. **21** (1953) 1975.
12. R. P. S. RATHORE, *Acta Physica Polonica* **A55** (1979) 637.
13. D. SINGH and R. P. S. RATHORE, *Phys. Stat. Sol*. (*b*) **170** (1992) 443.
14. R. HILL, *Proc. Phys. Soc. (Lond.)* **65** (1952) 349.

Received 22 March
and accepted 9 August 2000